

# Waveform inversion using a logarithmic wavefield

Changsoo Shin\*, Seoul National University, and Dong-Joo Min, Korea Ocean Research and Development Institute

## Summary

We propose a new objective function constructed by taking the logarithm of wavefields, which allows the separation of the objective function into three types using amplitude-only, phase-only and both. In our waveform inversion, we estimate the source signatures as well as the velocity structures by expressing the amplitudes and phases of the source signature in the objective function. We compute the steepest descent directions by using a matrix formalism derived from the frequency-domain finite-element/finite-difference modeling technique. Our numerical algorithms are similar to those of reverse-time migration and waveform inversion based on the adjoint state of the wave equation.

In order to demonstrate the practical applicability of our algorithm, we use a synthetic data set from the Marmousi model. For synthetic data, the velocity structure inverted by our inversion algorithm is more compatible with the true velocity structure than that of the conventional waveform inversion algorithm.

## Introduction

Since Lailly (1983) and Tarantola (1984) suggested that the backpropagation algorithm of reverse-time migration can be used in seismic inversion, their ideas have commonly been used in the time-domain traveltimes tomographic inversion and waveform inversion (Gauthier et al., 1986; Zhou et al., 1995). Pratt et al. (1998) applied the same idea to the frequency-domain waveform inversion, and showed that the backpropagation algorithm can be efficiently used for the waveform inversion of large-scale geological models. After that, the backpropagation algorithm began to be used frequently in frequency-domain traveltimes tomography and waveform inversion (Pratt, 1999; Hicks and Pratt, 2001).

According to Lailly (1983), prestack reverse-time migration can be regarded as the first iteration result of waveform inversion, so waveform inversion and prestack reverse-time migration share the numerical algorithm that originates from the symmetry of Green's function of the wave equation.

For a new waveform inversion algorithm, we devised an objective function using the logarithmic wavefield. By taking the logarithm of the wavefield, we can separate amplitude and phase, which allows us to construct three kinds of objective functions using amplitude-only, phase-only and both. In other words, we can invert the amplitude and the phase, either separately or simultaneously. Our waveform inversion algorithm also includes the inver-

sion of the source signature. In real seismic data, since the source signature is usually unknown, we need to estimate the source signature simultaneously (Pratt, 1999) with velocity inversion. With our separation of the objective function, it is possible to explicitly express the amplitude and the phase of the source signature in our objective function, therefore we can recover the amplitude and the phase of the source signature separately.

## Waveform inversion algorithm

We construct an objective function that is separable into three types (using amplitude-only, phase-only, and both), and adopt the principle of implicit calculation of the steepest descent direction (i.e., without directly computing Fréchet derivatives). This is accomplished by using the backpropagation technique of the reverse-time migration based on the adjoint state of the wave equation (e.g., Pratt et al., 1998).

For simplicity, we begin with a 1-D model. The 1-D constant density acoustic wave equation can be written as

$$\frac{\partial^2 u(z, t)}{\partial z^2} = \frac{1}{v(z)^2} \frac{\partial^2 u(z, t)}{\partial t^2} + f(z)g(t), \quad (1)$$

where  $v(z)$  is the subsurface velocity function,  $u(z, t)$  is the acoustic pressure field,  $f(z)$  is the source function in depth, and  $g(t)$  is the source function in time. In the frequency domain, we take the Fourier transform of equation (1) and then solve the discretized matrix equation using the frequency-domain finite-difference or finite-element modeling methods. In this case, we obtain the matrix equation (Marfurt, 1984)

$$\mathbf{S}(\omega)\tilde{\mathbf{u}}(\omega) = \mathbf{f}(z)g(\omega), \quad (2)$$

where  $\omega$  is the angular frequency,  $\mathbf{S}(\omega)$  is the complex impedance matrix,  $\tilde{\mathbf{u}}(\omega)$  is the Fourier-transformed wavefield,  $\mathbf{f}(z)$  is the source vector in depth and  $g(\omega)$  is the source function in the frequency domain. For simplicity, we write the complex source function  $g(\omega)$  of equation (2) as  $g_s(\omega) \exp[i\theta_s(\omega)]$ , yielding

$$\mathbf{S}(\omega)\tilde{\mathbf{u}}(\omega) = \mathbf{f}(z)g_s(\omega) \exp[i\theta_s(\omega)], \quad (3)$$

where  $g_s(\omega)$  and  $\theta_s(\omega)$  are the amplitude and the phase spectra of the source wavelet, respectively.

Suppose that the 1-D earth model is subdivided into a finite-difference grid in the  $z$ -direction [ $z = (j - 1)\Delta z$ ;  $j = 1, 2, \dots, N$ ] and each nodal point is parametrized with velocity  $p_k$  at the  $k$ th depth point. The 1-D wavefield at each frequency can be expressed as

$$\tilde{u}_j(\omega) = g_s(\omega)A_j^m(\omega) \exp[i\theta_j^m(\omega) + i\theta_s(\omega)], \quad (4)$$

where  $\tilde{u}_j(\omega)$  is the wavefield at the  $j$ th depth point,  $A_j^m(\omega)$  is the amplitude of the Green's function at the  $j$ th depth point,  $\theta_j^m(\omega)$  is the phase spectrum of the Green's function at the  $j$ th depth point, and  $\theta_s(\omega)$  is the phase spectrum of the source signature. The superscript  $m$  is used to discriminate modeled data from field data (which will be represented using the superscript  $f$ ). The modeled wavefield at the surface is

$$\tilde{u}_1(\omega) = g_s(\omega)A_1^m(\omega) \exp [i\theta_1^m(\omega) + i\theta_s(\omega)]. \quad (5)$$

Similarly, the measured field seismogram at the surface is

$$\tilde{d}_1(\omega) = A_1^f(\omega) \exp [i\theta_1^f(\omega)], \quad (6)$$

where  $\tilde{d}_1(\omega)$  is the wavefield measured at the surface, and  $A_1^f(\omega)$  and  $\theta_1^f(\omega)$  are the amplitude and the phase of the wavefield measured at the surface, respectively. However, when we extract the phase information from the measured or modeled wavefields, we actually obtain the wrapped phases (unless we apply an unwrapping algorithm). As a result, we rewrite equations (5) and (6) as

$$\tilde{u}_1(\omega) = g_s(\omega)A_1^m(\omega) \exp [i(\theta_1^m(\omega) + 2\pi n_m + \theta_s(\omega) + 2\pi n_s)] \quad (7)$$

and

$$\tilde{d}_1(\omega) = A_1^f(\omega) \exp [i(\theta_1^f(\omega) + 2\pi n_f)], \quad (8)$$

respectively, where  $n_m$ ,  $n_s$  and  $n_f$  are the arbitrary integers.

In our new waveform inversion algorithm, we construct an objective function based on the  $l_2$  norm of residuals between logarithmic modeled wavefields and field wavefields. By assuming that  $n_m + n_s = n_f$ , which means that the model is close to the true model, the objective function can then be defined for a single frequency as

$$E = \frac{1}{2} \left\{ \left[ \ln \frac{g_s(\omega)A_1^m(\omega)}{A_1^f(\omega)} \right]^2 + [\theta_1^m(\omega) + \theta_s(\omega) - \theta_1^f(\omega)]^2 \right\} \quad (9)$$

where the factor 1/2 is used to simplify the resulting equation. The gradient of this objective function with respect to the  $k$ th velocity parameter  $p_k$  is

$$\begin{aligned} \phi_k &= \nabla_{p_k} E = \frac{\partial E}{\partial p_k} \\ &= \ln \left( \frac{g_s(\omega)A_1^m(\omega)}{A_1^f(\omega)} \right) \left( \frac{1}{A_1^m(\omega)} \right) \frac{\partial A_1^m(\omega)}{\partial p_k} \\ &\quad + [\theta_1^m(\omega) + \theta_s(\omega) - \theta_1^f(\omega)] \frac{\partial \theta_1^m(\omega)}{\partial p_k}. \end{aligned} \quad (10)$$

A straightforward technique for calculating the gradient is to compute and use the partial derivative wavefield:

$$\frac{1}{\tilde{u}_1(\omega)} \frac{\partial \tilde{u}_1(\omega)}{\partial p_k} = \frac{1}{A_1^m(\omega)} \frac{\partial A_1^m(\omega)}{\partial p_k} + i \frac{\partial \theta_1^m(\omega)}{\partial p_k}. \quad (11)$$

We recognize that the terms on the right hand side of equation (10) can be obtained by taking the conjugate of

equation (11), multiplying it by equation (11), and taking the real part of the result. Thus,

$$\phi_k = Re \left\{ \left[ \ln \frac{\tilde{u}_1(\omega)}{\tilde{d}_1(\omega)} \right]^* \frac{1}{\tilde{u}_1(\omega)} \frac{\partial \tilde{u}_1(\omega)}{\partial p_k} \right\}, \quad (12)$$

where  $*$  indicates the complex conjugate. Equation (12) for an entire frequency band can be rewritten in matrix form as

$$\phi_k = Re \int_{-\infty}^{\infty} \left[ \frac{\partial \tilde{u}_1(\omega)}{\partial p_k} \quad \frac{\partial \tilde{u}_2(\omega)}{\partial p_k} \quad \dots \quad \frac{\partial \tilde{u}_N(\omega)}{\partial p_k} \right] \mathbf{r}(\omega) d\omega \quad (13)$$

with

$$\mathbf{r}(\omega) = \begin{bmatrix} \left[ \ln \frac{\tilde{u}_1(\omega)}{\tilde{d}_1(\omega)} \right]^* \\ \frac{1}{\tilde{u}_1(\omega)} \\ 0 \\ \vdots \\ 0 \end{bmatrix}. \quad (14)$$

By expressing the partial derivative wavefield by the virtual source  $\mathbf{v}_k$  and the modeling operator  $\mathbf{S}(\omega)$ , we obtain

$$\phi_k = Re \left\{ \int_{-\infty}^{\infty} \mathbf{v}_k^T(\omega) [\mathbf{S}^{-1}(\omega)]^T \mathbf{r}(\omega) d\omega \right\}, \quad (15)$$

and the entire steepest descent direction is

$$\phi = Re \left\{ \int_{-\infty}^{\infty} \mathbf{V}^T(\omega) [\mathbf{S}^{-1}(\omega)]^T \mathbf{r}(\omega) d\omega \right\}, \quad (16)$$

where  $\mathbf{V}$  is the virtual source matrix whose column is the virtual source vector  $\mathbf{v}_k$  at the  $k$ th depth point.

Since the modeling operator  $\mathbf{S}(\omega)$  is self adjoint,  $[\mathbf{S}^{-1}(\omega)]^T$  is interpreted as a backpropagation operator, and consequently the numerical structure of equation (16) is similar to that of reverse-time migration (Pratt et al., 1998; Shin et al., 2003). However, unlike the reverse-time migration in which the field data are backpropagated, we take the logarithmic residuals, divide them by the current model response at the surface, and backpropagate them in backward time. We obtain the steepest descent direction by calculating a zero-lag value of convolution between the backpropagated wavefield and the virtual source, as we normally do in the prestack reverse-time migration and prestack waveform inversion (Pratt et al., 1998).

When we compute the steepest descent direction of the objective function of the amplitude and the phase of the wavefield for the inversion, we can divide the objective function into three types using pure amplitude, pure phase, and both

## Numerical Examples

We test our waveform inversion algorithms on synthetic data generated for the IFP Marmousi data (Versteeg, 1994). Figure 1 shows the 16 m-grid Marmousi model.

To generate the synthetic seismograms of the Marmousi model, we used the 9-point, frequency-domain, finite-difference modeling technique suggested by Jo et al. (1996). We use the first derivative of Gaussian function with the maximum frequency of 18.41 Hz for the source wavelet.

We perform full waveform inversion employing both the amplitude and the phase based on equation (16). For an initial model for the inversion, we take a linearly increasing velocity model, where velocity varies from 1500 m/s to 4500 m/s as shown in Figure 2a. In Figure 2b, we present the velocity structure obtained by our full waveform inversion algorithm at the 1928th iteration. Since we use small step length, the convergence rate is very slow. We can accelerate convergence using other optimization techniques such as conjugate gradient method. In the inversion, we update the amplitude and the phase of the source wavelet at each iteration. In order to check the accuracy of our waveform inversion algorithm, we compare the velocity model inverted by our algorithm to that of the conventional, source-independent waveform inversion. For the conventional, source-independent inversion algorithm, we construct the objective function using the  $l_2$  norm of residuals between field data and model responses normalized by the reference wavefields. With the exception of the objective function, the numerical algorithm of the conventional inversion is the same as ours. Figure 2c shows the velocity structure generated by the conventional inversion algorithm. In Figure 2c, the left part of the inverted model is not accurately recovered.

In order to measure the sensitivity of the inversion results with respect to amplitude and phase, we also show the velocity models inverted by the pure amplitude method [equation (16)] at the 198th iteration and the pure phase method [equation (16)] at the 1253th iteration in Figures 3a and 3b, respectively. In each case, we invert either the amplitude or the phase of the source signature. From Figures 3a and 3b, we note that the pure phase method gives a velocity model comparable to that of the full waveform inversion method using both amplitude and phase, whereas the pure amplitude method does not yield good results.

## Conclusions

We built an objective function that can be separated into three types via the complex phase: the misfit of the amplitude, the misfit of the phase, and the misfit of both the amplitude and the phase. This separation leads to three kinds of inversions: the simultaneous inversion of amplitude and phase, pure amplitude inversion, or pure phase inversion. We estimated the source signature as well as the subsurface velocity by including the amplitude and the phase of the source signature in our objective function.

In our waveform inversion, we computed the steepest descent direction of the three different objective functions without directly computing the sensitivity matrix. The

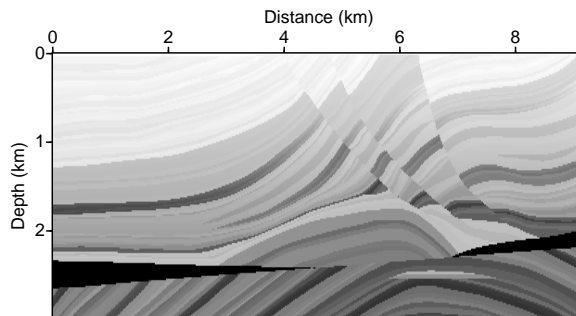


Fig. 1: The 2-D IFP Marmousi model.

steepest descent direction is computed by the backpropagation algorithm of the reverse-time migration on the basis of the matrix formalism of the frequency-domain finite-element/finite-difference method for the wave equation. Our algorithm shares the same numerical algorithm with prestack reverse-time migration and seismic inversion.

By applying three inversion algorithms to the synthetic seismogram of the Marmousi model, we ensured that the simultaneous inversion of the amplitude and the phase produces the best resolution in the shallow and the deep structure of the Marmousi model.

## Acknowledgement

This work was financially supported by National Laboratory Project of Ministry of Science and Technology, and Brain Korea 21 project of Ministry of Education.

## References

- Gauthier, O., Virieux, J., and Tarantola, A., 1986, Two-dimensional nonlinear inversion of seismic waveforms: Numerical results: *Geophysics*, **51**, 1387-1403.
- Jo, C. H., Shin, C., and Suh, J. H., 1996, Design of an optimal 9 point finite difference frequency-space acoustic wave equation scheme for inversion and modeling: *Geophysics*, **61**, 329-337.
- Lailly, P., 1983, The seismic inverse problem as a sequence of before stack migration, in Bednar, J.B., Rednar, R., Robinson, E., and Weglein, A., Eds., *Conference on inverse Scattering: Theory and Application*, Soc. Industr. Appl. Math.
- Marfurt, K. J., 1984, Accuracy of finite-difference and finite-element modeling of the scalar and elastic wave equation: *Geophysics*, **49**, 533-549.
- Pratt, R. G., Shin, C. and Hicks, G. J., 1998, Gauss-Newton and full Newton methods in frequency domain seismic waveform inversion: *Geophys. J. Internat.*, **133**, 341-362.

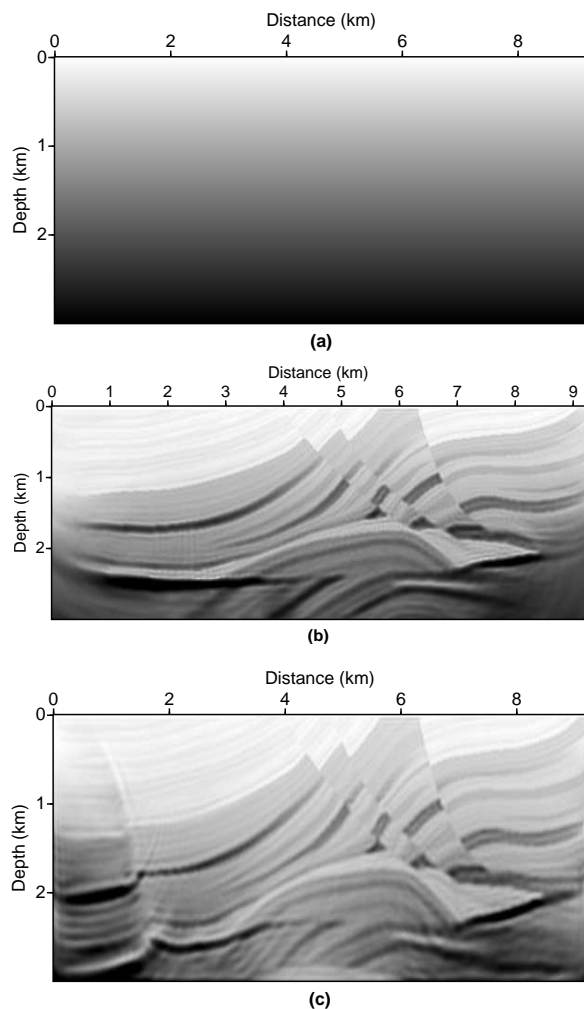


Fig. 2: Numerical examples for the noise-free Marmousi synthetic data: (a) the initial model, (b) the velocity model inverted by the full waveform inversion using both amplitude and phase at the 1928th iteration, and (c) the velocity model inverted by the conventional source-independent inversion algorithm at the 259th iteration.

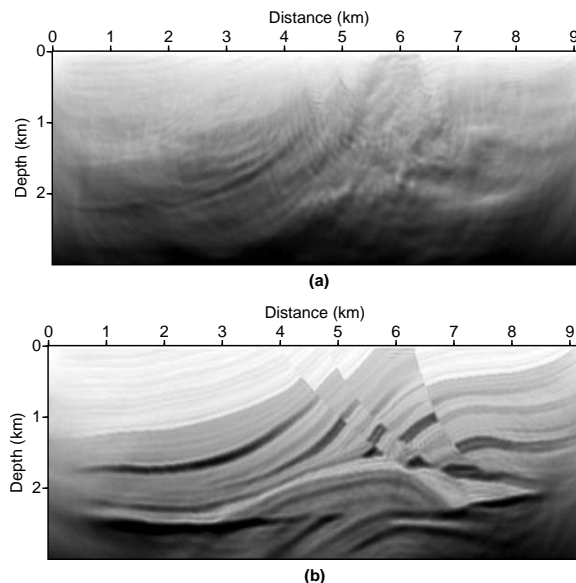


Fig. 3: The velocity structures generated for the noise-free Marmousi synthetic data by (a) the pure amplitude inversion method at the 198th iteration and (b) the pure phase inversion method at the 1253th iteration.

Pratt, R. G., 1999, Seismic waveform inversion in the frequency domain, Part 1: Theory and verification in a physical scale model: *Geophysics*, **64**, 888-901.

Shin, C., Min, D. J., Yang, D. W., and Lee, S. K, 2003, Evaluation of post stack migration in terms of virtual source and partial derivative wavefields: *Journal of Seismic Exploration*, **12**, 17-37.

Tarantola, A., 1984, Inversion of seismic reflection data in the acoustic approximation: *Geophysics*, **49**, 1259-1266.

Versteeg, R., 1994, The Marmousi experience: Velocity model determination on a synthetic complex data set: *The Leading Edge*, **13**, 927-936.

Zhou, C., Cai, W., Luo, Y., Schuster, G. T., and Hasanzadeh, S., 1995, Acoustic wave equation traveltime and waveform inversion of cross hole seismic data: *Geophysics*, **60**, 765-773.